

On the Motions of High Speed Surface-Effect-Ship in Waves

G.J. Lee¹

Abstract

The motion response of a high speed SES in waves is important because the ride quality of passengers is mainly affected by it. The pitch motion has a large influence on the vertical motion at the bow. But the pitch motion of SES does not have been analyzed properly. The reason for that is the absence of proper mathematical model for the stern bag, the bow seal, and the inherent non-linearity.

In this paper, the heave and pitch motion of high speed SES in waves have been treated. For doing it, the mathematical model for the stern bag was set up, and the hydrodynamic forces on the side hulls were obtained by using the principle of momentum change. The motion responses in waves were calculated, and the analysis of the motions was done.

1 Introduction

The SES(Surface Effect Ship) has been proved to be adequate for a high-speed passenger ship because of its speed and relatively good seakeeping quality[1]. An SES has some advantages compared with an ACV such as the directional stability, less power of lift fan, water-born propulsion device etc. because of its side hulls. Compared with the other types of the high speed passenger ships in service such as the hydro-foil ship and the catamaran, the seakeeping quality of SES especially in the acceleration level for high encounter frequency, is relatively good because of its air cushion effect. The vertical motions and their associated accelerations are known to have important influence on the human habitability in a seaway. So, many studies relating the RCS(ride control system) were done[1,2,3,4,5] to reduce these motions. As the speed of craft becomes high, the acceleration grows very high although the displacement does not grow, because the encountering frequency of waves becomes high.

Especially at the bow and the stern, the vertical motion is affected by not only the heave motion but also the pitch motion to a large extent. But the previous studies are mainly concentrated on the heave motion, not on the pitch motion. The reason for that is the absence of proper mathematical model for the stern bag, the bow seal, and the inherent non-linearity. In order to analyze the pitch motion, we must know the deformation and

¹Member, Research Engineer in Post Doctoral Program, Seoul National University

dynamic model of the stern bag and also the hydrodynamics of the side hulls. Usually the shape of the side hull is similar to that of a planning boat, so the hydrodynamics can be analyzed by using the principle of the momentum change, which has been used successfully and extensively in the problem of the high speed planning boats[6,7,8]. The deformation model and hydrodynamics of the bag has been studied recently[9,10,11,12], however there are many problems in applying the results to the dynamics of the high speed SES, especially in the dynamic matching between the bag and the craft.

In this paper, the heave and pitch motions of a high speed SES in waves are treated. A mathematical model on the deformation of the stern bag is set up, and the effect of the stern bag on the pitch motion is analyzed. On the side hulls, the hydrodynamic forces are obtained by using the principle of the momentum change that is used extensively on the hydrodynamic problems of planning boats. The equations of motion consist of 6 modes: heave, pitch and 4 pressure variations. The motion responses are obtained in the time domain, because the dynamics of SES has the inherent non-linearity. The motion responses of SES in regular and in irregular waves are computed. The analyses of the effect of the stern bag on the pitch motion, the bow and stern acceleration, force components during the motion, and the degree of the non-linearity have been done.

2 Equations of Motion of SES

Consider a SES(Surface Effect Ship) advancing forward with a constant speed U . The shape of SES is shown in Fig.1, and the coordinate systems in Fig.2. The right handed coordinate systems are adopted, and the x -axis lies in the forward direction and the z -axis upward.

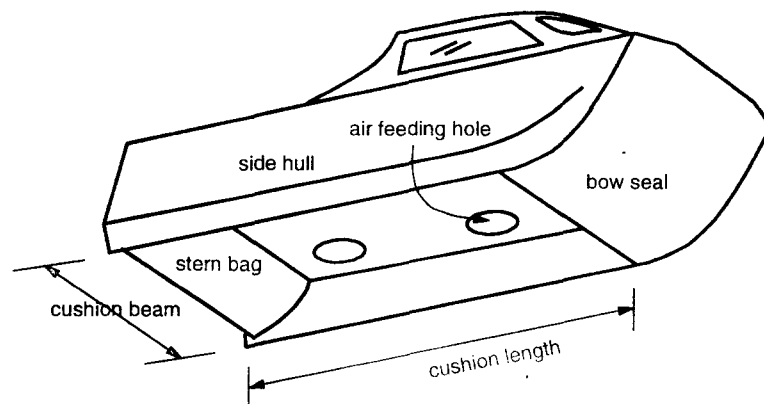


Figure 1: Surface Effect Ship

The forces acting on SES in waves mainly consist of the pressure force in the cushion chamber, bow seal, stern bag, and the hydrodynamic forces on the side hulls. For a low

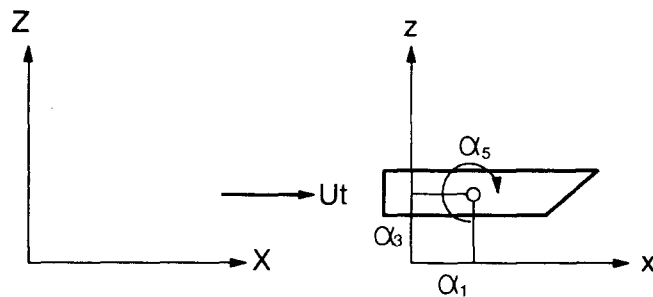


Figure 2: Coordinate Systems

forward speed, the free surface deformation due to pressure have to be considered and incorporated with the motion of the craft. But if the forward speed is very high, the free surface deformation generated by the cushion pressure is developed mainly in the down stream, Near the craft the free surface deforms small enough, so that the free surface elevation due to the cushion pressure is negligible.

Discussions are made for the forces acting on the cushion, on the side hull and on the seals. Then the mathematical model of the stern bag, and the equations of motion are considered.

2.1 Forces acting on the Side Hulls

The frequency dependent hydrodynamic forces take place when there exist free surface and the memory effect, which is induced by pressure variations in water due to the waves made by previous motions of a craft. So only when a body is in the wave field that is made by itself, the frequency dependent terms arise. Suppose that a craft is running forward at very high speed, then the craft displaces the water with its volume and the displaced water is running down aftward very quickly. In this case, the waves due to the craft are developed mainly in the down stream, and the frequency dependency for the hydrodynamics of the oscillating craft becomes smaller as the speed of a craft becomes larger. For the analysis of the motions of a relatively low speed craft in a regular wave, the frequency dependent hydrodynamic phenomena must be considered. Even in a regular wave, the non-linear motion creates different frequency components, so the analysis will be made using a harmonics analysis. In irregular waves, the number of harmonics to be calculated becomes so large that the harmonic analysis is no more practical. Therefore, it is practical that the motions of a high speed craft in irregular waves are calculated by using only the frequency independent forces.

Many researchers used the principle of the momentum change to calculate the hydrodynamic forces acting on a planing boat, and the results agreed well with experimental ones.[6,7,8] In this paper, the method of momentum change will be used to calculate the forces acting on the side hulls.

First, consider the relative velocity between the fluid and the body. At a position whose

x coordinate is r , the displacement can be written as

$$\begin{aligned} X &= U_0 t + \alpha_1 + r \cos \alpha_5, \\ Z &= \alpha_3 - r \sin \alpha_5. \end{aligned} \quad (1)$$

The velocity normal to the base line can be obtained as follows.

$$\begin{aligned} V_B &= \dot{X} \sin \alpha_5 + \dot{Z} \cos \alpha_5 \\ &= \dot{\alpha}_3 \cos \alpha_5 + (\dot{\alpha}_1 + U_0) \sin \alpha_5 - r \dot{\alpha}_5 \end{aligned} \quad (2)$$

The normal velocity due to the waves is

$$V_W = u_W \sin \alpha_5 + w_W \cos \alpha_5, \quad (3)$$

where u_W, w_W are the fluid velocities of the waves in the direction of x and z respectively. The relative velocity viewed from the moving craft is as follows.

$$\begin{aligned} V_r &= V_W - V_B \\ &= (w_W - \dot{\alpha}_3) \cos \alpha_5 + (u_W - \dot{\alpha}_1) \sin \alpha_5 - U_0 \sin \alpha_5 + r \dot{\alpha}_5. \end{aligned} \quad (4)$$

Let's consider the forces due to the momentum change. The normal force component acting on the hull at a certain section can be represented as

$$dF = \frac{d}{dt}(m_a V_r) = \dot{m}_a V_r + m_a \dot{V}_r - U_0 \frac{\partial}{\partial x}(m_a V_r). \quad (5)$$

The force can be calculated by integrating the above force component.

$$F_m = \int dF = \int (\dot{m}_a V_r + m_a \dot{V}_r) dr - \frac{U_0}{\cos \alpha_5} [m_a V_r]_A^F \quad (6)$$

And the moment is

$$\begin{aligned} M_m &= - \int r dF = - \int (\dot{m}_a V_r + m_a \dot{V}_r) r dr + U_0 \int r \frac{\partial}{\partial x} (m_a V_r) dr \\ &= - \int (\dot{m}_a V_r + m_a \dot{V}_r) r dr + \frac{U_0}{\cos \alpha_5} \left\{ [r m_a V_r]_A^F - \int m_a V_r dr \right\}. \end{aligned} \quad (7)$$

The added mass m_a is a function of the water surface height from the base line. The time rate of height and added mass are

$$\begin{aligned} h &= h_0 + \zeta_W - (\alpha_3 - r \sin \alpha_5) \\ \dot{h} &= \dot{\zeta}_W - (\dot{\alpha}_3 - r \cos \alpha_5 \dot{\alpha}_5). \end{aligned} \quad (8)$$

$$\dot{m}_a = \frac{\partial m_a}{\partial h} \cdot \dot{h}, \quad \text{if } h < 0 \quad \begin{cases} m_a = 0, \\ \frac{\partial m_a}{\partial h} = 0. \end{cases} \quad (9)$$

Let's divide the relative acceleration dV_r/dt into the craft's acceleration and the others.

$$\begin{aligned}\dot{V}_r &= a_r - \ddot{\alpha}_3 \cos \alpha_5 + r\ddot{\alpha}_5 - \ddot{\alpha}_1 \sin \alpha_5 \\ a_r &= \dot{w}_W \cos \alpha_5 + \dot{u}_W \sin \alpha_5 \\ &\quad - (w_W - \dot{\alpha}_3) \sin \alpha_5 \dot{\alpha}_5 + (u_W - \dot{\alpha}_1) \cos \alpha_5 \dot{\alpha}_5 - U_0 \cos \alpha_5 \dot{\alpha}_5\end{aligned}\quad (10)$$

Then the force and moment can be rewritten as

$$\begin{aligned}F_m &= -(\ddot{\alpha}_3 \cos \alpha_5 + \ddot{\alpha}_1 \sin \alpha_5) \int m_a dr + \ddot{\alpha}_5 \int m_a r dr \\ &\quad + \int \left(\frac{\partial m_a}{\partial h} \dot{h} V_r + m_a a_r \right) dr - \frac{U_0}{\cos \alpha_5} [m_a V_r]_A^F, \\ M_m &= +(\ddot{\alpha}_3 \cos \alpha_5 + \ddot{\alpha}_1 \sin \alpha_5) \int m_a r dr - \ddot{\alpha}_5 \int m_a r^2 dr \\ &\quad - \int \left(\frac{\partial m_a}{\partial h} \dot{h} V_r + m_a a_r \right) r dr + \frac{U_0}{\cos \alpha_5} \left\{ [r m_a V_r]_A^F - \int m_a V_r dr \right\}\end{aligned}\quad (11)$$

Similarly, the damping force independent to frequency will be considered. Zarnick & Long-Wen[7] used the cross flow drag for the damping force.[8]

$$\begin{aligned}dF_d &= C_D \rho b V_r |V_r| \\ F_d &= C_D \rho \int b V_r |V_r| dr \\ M_d &= -C_D \rho \int b V_r |V_r| r dr\end{aligned}\quad (12)$$

The restoring force can be calculated as follows,

$$F_R = \rho g \int S dr, \quad M_R = -\rho g \int S r dr. \quad (13)$$

where S is the submerged area at a certain section. The integral appeared in this section must carry on only along the portion of side hull in which the water surface height is positive.

2.2 Air Flows and the Pressure Forces

The air flows and the variables used for this formulation are shown in Fig.3.

The expansion process of the air is assumed to follow the adiabatic process. The state equation of the air in the adiabatic process is represented by the following equation.

$$\rho = \rho_a \left(\frac{p}{p_a} \right)^{1/\gamma} \quad (14)$$

where p_a is the atmospheric pressure, ρ_a is the density of air at 1 atm, and γ is the specific heat. Hereafter the pressure will be recognized as the absolute pressure. The governing equations of air flow can be set up by applying the mass conservation law at the four

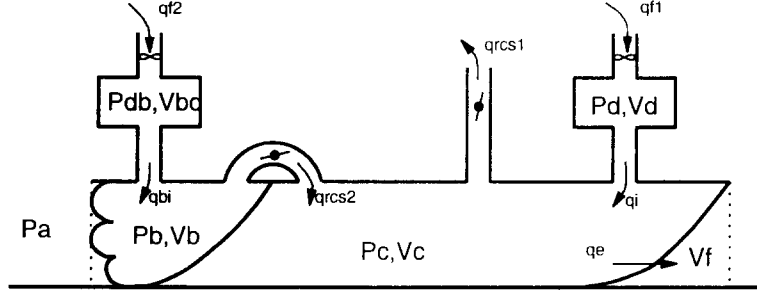


Figure 3: The Air Flows

locations, those are the cushion chamber, duct, stern bag and the duct for bag. The volume of the cushion chamber and the stern bag may be changed when the craft oscillates and the incoming waves are present.

The mass conservation law of air in the cushion chamber can be written as

$$\frac{d}{dt}(\rho_c V_c) = \dot{\rho}_c V_c + \rho_c \dot{V}_c = q_i + q_{RCS2} - q_e - q_{RCS1}, \quad (15)$$

where the variable q is the mass flux. Using the state equation of air Eq.(14), the above equation can be rewritten as follows.

$$\frac{\rho_c V_c}{\gamma p_c} \dot{p}_c = q_i + q_{RCS2} - q_e - q_{RCS1} - \rho_c \dot{V}_c \quad (16)$$

Similarly, the mass conservation laws in the duct, stern bag, duct for the stern bag are

$$\begin{aligned} \frac{\rho_d V_d}{\gamma p_d} \cdot \dot{p}_d &= -q_i + q_{f1}, \\ \frac{\rho_b V_b}{\gamma p_b} \cdot \dot{p}_b &= q_{bi} - q_{RCS2} - \rho_b \dot{V}_b, \\ \frac{\rho_{bd} V_{bd}}{\gamma p_{bd}} \cdot \dot{p}_{bd} &= q_{f2} - q_{bi}. \end{aligned} \quad (17)$$

If there is no duct, the above equations are reduced as the following two equations.

$$\begin{aligned} \frac{\rho_c V_c}{\gamma p_c} \dot{p}_c &= q_{f1} + q_{RCS2} - q_e - q_{RCS1} - \rho_c \dot{V}_c \\ \frac{\rho_b V_b}{\gamma p_b} \dot{p}_b &= q_{f2} - q_{RCS2} - \rho_b \dot{V}_b \end{aligned} \quad (18)$$

To solve the above equations, varying volume V_c, V_b must be known. The deformation model and the volume of the stern bag are given in section 2.3. The volume of the cushion chamber may be calculated when the wave elevation and the motion of SES are given.

$$V_c = \iint z_d dx dy - V_b - V_f, \quad (19)$$

where V_f is the volume between the plane drawn vertically from the bow to the free surface and the bow seal. The distance between the free surface and the upper plate of the cushion chamber z_d is

$$z_d = z_0 + \alpha_3 - x\alpha_5 - \zeta_W \quad (20)$$

The mass flux q can be calculated by using the following orifice equations.

$$\begin{aligned} q_i &= kA_i\rho_d\sqrt{2(p_d - p_c)/\rho_d} \\ q_{bi} &= kA_{bi}\rho_{bd}\sqrt{2(p_{bd} - p_b)/\rho_{bd}} \\ q_{RCS1} &= kA_{RCS1}\rho_c\sqrt{2(p_c - p_a)/\rho_c} \\ q_{RCS2} &= kA_{RCS2}\rho_b\sqrt{2(p_b - p_c)/\rho_b} \\ q_e &= kA_e\rho_c\sqrt{2(p_c - p_a)/\rho_c} \end{aligned} \quad (21)$$

where the contraction coefficient k is chosen as 0.65, the data A 's are the inlet and outlet areas. The outlet area A_e depends on the motions of craft and waves. It consists of the gap between the lower part of the craft and water surface, and seal system itself. The air tightness of cushion chamber is not perfect, so the leakage will take place even when no motion occurs. This leakage area is to be considered as the outlet area A_{e0} .

$$A_e = A_{e0} + \int_{\text{Side Hull}} g_S dl + \int_{\text{Stern Bag}} g_B dl + \int_{\text{Bow Seal}} g_F dl, \quad (22)$$

where g_S, g_B, g_F are the gaps between the free surface and the lowest point of side hull, stern bag, bow seal respectively. The air feedings q_{f1}, q_{f2} are governed by the characteristics of the feeding fan. The relationship between the pressure difference and air flux is assumed to obey the following equation.

$$\Delta p_{fi} = \begin{cases} C_{0i} + C_{1i}q_{fi} & \text{if } \Delta p_{fi} > C_{2i} \\ C_{2i} + C_{3i}(q_{fi} - q_{fi}^*) & \text{if } \Delta p_{fi} < C_{2i} \end{cases} \quad \text{for } i = 1, 2, \quad (23)$$

where Δp_{fi} is the pressure difference across the fan and q_{fi} is the mass flux. And q_{fi}^* is the mass flux when $\Delta p_{fi} = C_{2i}$.

The forces acting on the craft due to the pressure is the same in magnitude and opposite in direction to the pressure forces acting on the free surface. Therefore the area of pressure patch exposed to free surface and the center of area must be known. The force and moment acting on the craft are

$$\begin{aligned} F_p &= A_c p_c + A_b p_b, \\ M_p &= -x_c A_c p_c - x_b A_b p_b, \end{aligned} \quad (24)$$

where A_c, A_b are the area of cushion and stern bag exposed to the free surface respectively, and x_c, x_b the centers. These are not fixed but varying at each time. The area A_c is the cushion area enclosed from the point at which the bag starts to meet the free surface or the lowest point of the bag, to the point at which the bow seal meets the free surface. So the force of the bow seal is automatically included in the above Eq.(24) in the form of the cushion area.

2.3 Mathematical Model of the Stern Bag

The stern bag of SES prevents the air leakage from the cushion chamber, usually it is made of fiber so that it can be deformed easily by the free surface. The free surface deformation due to the cushion pressure is small near the stern bag if the speed of SES is high. Therefore the free surface is assumed to be rigid. The shape of a bag is given in Fig.4 and Fig.5.

In calculations of the shape of a bag, the slope of the free surface θ_W is included in θ ,

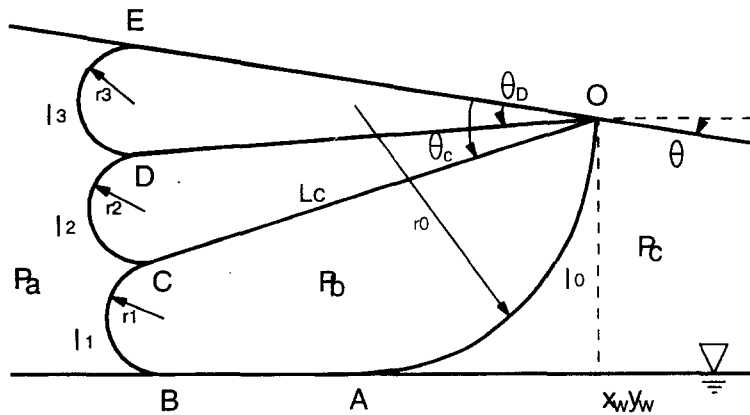


Figure 4: Shape of a Stern Bag and Parameters



Figure 5: Normal and Overlapped Shape at Point C

so that $\theta = \alpha_5 + \theta_W$ where α_5 is the pitch angle of SES. The sign convention of θ_W is positive when the surface goes up as x increases. Then the free surface can be considered as the horizontal surface. Assume that the pressures, the lengths of each segment of a bag, and the free surface are given. To obtain the shape and area of the bag, the following assumptions are made.

1. The length of each segment is constant.
2. OE, OD, OC are straight and the same in length.
3. At the point A,B, the bag meets the free surface tangentially.

4. In all the arcs of the bag, the Laplace formula (relationship of pressure, tension, and radius of curvature) must hold.
5. All segments transmit the tension, not moment.
6. All segments are assumed to be massless.

The shape of the bag can be totally obtained, provided that the four unknowns x_A, x_B, θ_C, l_1 (l_1 may be interchanged with l_0 if necessary.) have been solved. The parameter used to find the shape of the bag can be calculated as below using four unknowns.

$$\begin{aligned}
 \theta_D &= \theta_C/2 \quad , \quad y_B = y_A = y_w \\
 x_E &= -L_c \cos(-\theta) \quad , \quad y_E = -L_c \sin(-\theta) \\
 x_D &= -L_c \cos(\theta_D - \theta) \quad , \quad y_D = -L_c \sin(\theta_D - \theta) \\
 x_C &= -L_c \cos(\theta_C - \theta) \quad , \quad y_C = -L_c \sin(\theta_C - \theta)
 \end{aligned} \tag{25}$$

$$\begin{aligned}
 \beta_{C1} &= \tan^{-1}(y_C - y_B, x_C - x_B) - \theta_C - \frac{1}{2} \frac{l_1}{r_1} \\
 \beta_{C2} &= \pi - \tan^{-1}(y_D - y_C, x_D - x_C) + \theta_C - \frac{1}{2} \frac{l_2}{r_2}
 \end{aligned} \tag{26}$$

$$l_0 = L - l_1 - \overline{AB} \tag{27}$$

$$\frac{\overline{CD}}{2r_2} = \sin \frac{l_2}{2r_2} \quad , \quad \frac{\overline{BC}}{2r_1} = \sin \frac{l_1}{2r_1} \quad , \quad \frac{\overline{OA}}{2r_0} = \sin \frac{l_0}{2r_0} \tag{28}$$

where Eq.(28) are for the radii provided that the length and distance between two points are given. However, these are not the closed forms, so the radii should be obtained by iteration method.

The four unknowns are governed by the following four conditions: first two conditions are that the bag meets the free surface tangentially at the points A and B, the third condition represented the tension relation in the segment OABC, and the last condition the force equilibrium at the point C.

$$\begin{aligned}
 f_1 &= \tan^{-1}(y_O - y_A, x_O - x_A) - \frac{l_0}{2r_0} = 0 \\
 f_2 &= \tan^{-1}(y_C - y_B, x_C - x_B) + \frac{l_1}{2r_1} - \pi = 0 \\
 f_3 &= \frac{p_b - p_c}{p_b - p_a} r_0 - r_1 - \frac{\rho}{2(p_b - p_a)} C_f U^2 \overline{AB} = 0 \\
 f_4 &= r_2 \sin \beta_{C2} - r_1 \sin \beta_{C1} = 0.
 \end{aligned} \tag{29}$$

where C_f is the friction drag coefficient and U is the speed of SES. The four unknowns can be obtained from the above equations by Newton-Raphson method with a number of parameters given in Eq.(25), (26), (27), (28). This iteration does not converge when

$p_c > p_b$, but as the pressure in the cushion chamber increases and approaches the pressure in the bag, \overline{AB} tends to be zero and the bag flies above the free surface. Therefore the solution when the bag flies is needed, and at this time the decreasing pressure in the cushion chamber makes no problem in solving the above equations.

When the bag totally flies above the free surface, the special treatment is needed. If the bag flies above the free surface, we assume that the pressure on the portion of the bag before the lowest point is p_c , and behind the lowest point p_a . At this time the unknowns must be changed with x_A, y_A, θ_C, l_1 , and the point B coincides with the point A. The solution method is the same as mentioned previously. During the iteration, the bag is assumed fly if the point A is located behind the point B. And for the case that the bag goes down from the flying position, the bag is assumed to meet the free surface if y_A is lower than the free surface.

When the bag overlaps with itself, the special treatment is needed also. If the bag overlaps at the point C, the condition f_4 should be changed as follows.

$$f_4 = -l'_2 + l'_1 = 0 \quad (30)$$

where l'_1, l'_2 are the overlapped lengths in the segments BC and CD respectively. In this case, the angles β_{C1}, β_{C2} vanish. When overlapping happens, the shape near the overlapped point is changed, the equations to represent the shape and the criteria for overlapping is somewhat lengthy for explanation, so these explanations are omitted.

The area of the bag can be divide into the areas of inner hexapolygon and four arcs. The sum of areas of four arcs is

$$A_{arc} = \sum_{i=0}^3 (\theta_i - \sin \theta_i \cos \theta_i) r_i^2, \quad (31)$$

$$\theta_i = \frac{l_i - l'_i}{2r_i} \quad \text{for } i = 0, 1,$$

$$\theta_i = \frac{l_i - 2l'_i}{2r_i} \quad \text{for } i = 2, 3.$$

The area of the hexapolygon is

$$A_{poly} = \frac{y_0 + y_5}{2} (x_0 - x_5) + \sum_{i=0}^4 \frac{y_i + y_{i+1}}{2} (x_{i+1} - x_i), \quad (32)$$

where x_i, y_i are the positions of the points O,A,B,C,D,E according to $i=0,1,2,3,4,5$. The volume of the bag is the breadth of SES times the sum of Eq.(31) and (32). The area that the meet the free surface is \overline{AB} times the breadth of SES, and the center position is the mid point of \overline{AB} .

$$\begin{aligned} V_b &= b \cdot (A_{arc} + A_{poly}) \\ A_b &= b \cdot \overline{AB} \\ x_b &= (x_A + x_B)/2, \end{aligned} \quad (33)$$

where b is the cushion breadth of SES. These are used in the equations of motion of SES. As seen before, the shape of the bag can be obtained totally in the static manner. In order to apply this deformation model into the dynamics of SES, we must know the time rate of change of the volume. But the volume is determined in static manner, so we have no choice but differentiating the volume in numerical sense to obtain the time rate of change. Because the numerical differentiation amplify any numerical or truncation error to a large extent, the following filtered numerical scheme is adopted.

$$\begin{aligned} f_i &= \frac{V_b}{V_e} \\ \bar{f}_i &= e^{-\Delta t/\tau} \bar{f}_{i-1} + (1 - e^{-\Delta t/\tau}) f_i \\ \dot{V}_b &= \frac{d}{dt}(f \cdot V_e) = \frac{\bar{f}_i - \bar{f}_{i-1}}{\Delta t} V_e + f_i \dot{V}_e, \end{aligned} \quad (34)$$

where i is the index of the time step, and V_e is the volume enclosed by the plane which is drawn vertically from the point O to the free surface and by the plane drawn from the point E to the free surface vertically. V_e and \dot{V}_e can be obtained if the free surface elevation and the motion of craft are given. \bar{f} is the filtered value of the volume fraction f using the 1st order filter, which is characterized by the time constant τ .

2.4 Equations of motions

The equations of motion consist of the mass conservation laws in cushion chamber, duct, bag, duct for bag and the 6-degree of freedom equations of SES. In this paper, only heave and pitch equations are studied among 6 modes. The equations of motion for heave and pitch are represented as follows,

$$\begin{aligned} m\ddot{\alpha}_3 - mx_G\ddot{\alpha}_5 &= -mg + F_m + F_d + F_r + F_p, \\ I_5\ddot{\alpha}_5 - mx_G\ddot{\alpha}_3 &= mx_Gg + M_m + M_d + M_r + M_p, \end{aligned} \quad (35)$$

where m is the mass of SES, x_G the x coordinate of the center of gravity, I_5 the mass moment of inertia. There are forces proportional to the accelerations of the craft in F_m, M_m , we may rewrite the above equations using Eq.(11),

$$\begin{aligned} (m + a_{33})\ddot{\alpha}_3 + (-mx_G + a_{35})\ddot{\alpha}_5 &= -mg + F_h + F_d + F_r + F_p, \\ (-mx_G + a_{53})\ddot{\alpha}_3 + (I_5 + a_{55})\ddot{\alpha}_5 &= mx_Gg + M_h + M_d + M_r + M_p, \end{aligned} \quad (36)$$

where a 's are the added masses of the craft and the subscripts mean the force direction and the motion mode. The added masses are

$$\begin{aligned} a_{33} &= \cos \alpha_5 \int m_a dr, & a_{35} &= - \int m_a r dr, \\ a_{53} &= - \cos \alpha_5 \int m_a r dr, & a_{55} &= \int m_a r^2 dr, \end{aligned} \quad (37)$$

on the main dynamic behavior should not be significant. The original ship has been in her service since 1990. The specifications of the model is listed in the Table 1. The shape of side hull is also modified to a simple form as in Fig.6. And the dimensions are listed in the Table 2.

All calculations were made in double precision using a 386 based PC. The solution of the equations of motion was obtained in the time domain. The time interval Δt was set to 0.002 second. Because of the presence of the bag, the time interval is set relatively short. If there is no bag the time interval can be set to more large value, say 0.01-0.02 second.

Table 1. Specifications of the model used in calculation

Principal Dimensions			
m	154,000 kg	I_5	9,856,000 kg-m ²
l	32 m	b	8 m
x_G	-2.4 m	z_G	1 m
h_{seal}	3 m	l_{seal}	3 m
z_0	2 m		
Fan Characteristics			
Fan No. 1		Fan No. 2	
C_{01}	7500	C_{02}	10500
C_{11}	-50	C_{12}	-100
C_{21}	5000	C_{22}	7500
C_{31}	-100	C_{32}	-250
q_{f1}^*	50	q_{f2}^*	30
Bag Dimensions			
x_{bag}	-11.5 m	$L = l_0 + l_1 + AB$	7.5 m
L_c	4.5 m	l_2	1.5 m
l_3	1.5 m		
Data for Air Flows			
V_d	30 m ³	V_{bd}	10 m ³
p_{c0}	105000 Pa	p_{b0}	107500 Pa
A_i	0.98248 m ²	A_{bi}	0.76100 m ²
A_{RCS1}	0.70000 m ²	A_{RCS2}	0.58944 m ²
A_{e0}	0.41150 m ²		
Miscellaneous			
τ	0.02	γ	1.4
C_D	1.0	C_f	0.04

Before the calculation of the motion in waves, the initial state should be computed when the craft is running on the calm sea. This state can be computed by calculating the motion with no wave until the steady values are obtained. The results are : heave = 0.1025 m, pitch = -1.06 degree(bow down positive). $p_c = 104948$ Pa, $p_b = 107393$ Pa.

In all the cases, the direction of wave is set to be opposite to that of the craft, that is to say, head sea. Motions in a regular wave are plotted vs. the encountering frequency, *i.e.* frequency responses in many cases. Because all calculations are made by using non-linear

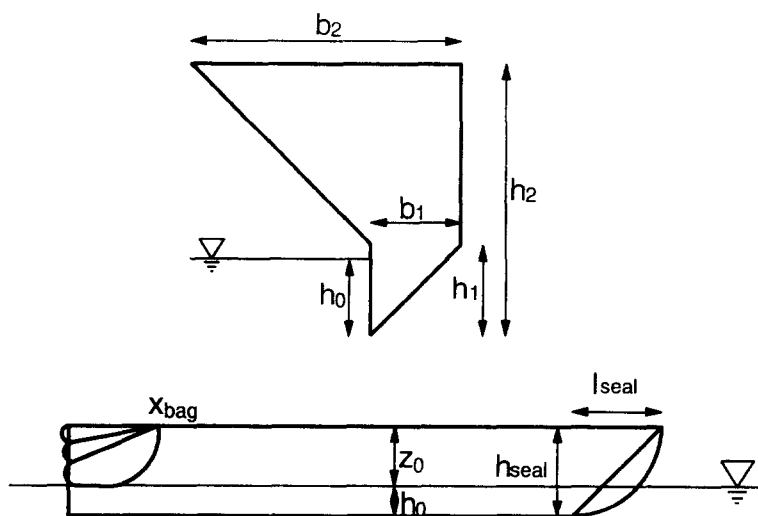


Figure 6: The Shape of Hulls

equations, the results are not sinusoidal. So the frequency responses were represented by the peak-to-peak value of the time domain solution after the steady solution seems to be obtained at each frequency. In addition, the 1st, 2nd, 3rd harmonic amplitudes is also computed. Let $f(t)$ be a time domain solution, the n-th harmonic amplitudes are computed as in the following equations.

$$A_n = \sqrt{A_{nC}^2 + A_{nS}^2} \quad (42)$$

$$A_{nC} = \frac{\omega_e}{\pi} \int_0^{\frac{2\pi}{\omega_e}} f(t) \cos n\omega_e t dt$$

$$A_{nS} = \frac{\omega_e}{\pi} \int_0^{\frac{2\pi}{\omega_e}} f(t) \sin n\omega_e t dt$$

It is convenient to define the 'distortion ratio' that represents the degree of the non-linearity.

$$r_D = \frac{\sqrt{A_2^2 + A_3^2}}{A_1} \quad (43)$$

Of course the numerator can be summed to higher order harmonics, but the above seems to be enough. If the time domain solution is purely sinusoidal as in the linear case, the half of peak-to-peak value is the same as A_1 , and A_2, A_3 vanish, so r_D equals to zero.

In the case of irregular wave, the surface elevation is generated by summing up 10 wave components which have random phases at initial state. The amplitude of the motions is represented as RMS(Root Mean Square) value.

3.1 Motions in Regular Wave

For a regular wave, 4 wave systems are selected, whose kA , the maximum wave slope, is 0.01, 0.05, 0.1, and 0.15.

Table 2. Data for the Side Hulls (in [m])

Station x	h_0	h_1	$b_{\max 1}$	h_2	$b_{\max 2}$
-16	1.0	1.0	1.0	3.0	3.0
-14	1.0	1.0	1.0	3.0	3.0
-12	1.0	1.0	1.0	3.0	2.9
-10	1.0	1.0	1.0	3.0	2.8
-8	1.0	1.0	1.0	3.0	2.6
-6	1.0	1.0	1.0	3.0	2.5
-4	1.0	1.0	1.0	3.0	2.3
-2	1.0	1.0	1.0	3.0	2.1
0	1.0	1.0	1.0	3.0	2.0
2	1.0	1.0	1.0	3.0	1.9
4	1.0	1.0	1.0	3.0	1.8
6	1.0	1.0	1.0	3.0	1.6
8	1.0	1.0	1.0	3.0	1.4
10	1.0	1.0	0.8	3.0	1.2
12	1.0	1.0	0.6	3.0	1.0
13	0.75	1.0	0.5	3.0	1.0
14	0.5	1.0	0.4	3.0	1.0
16	0.0	1.0	0.2	3.0	1.0

In Fig.7, the heave and pitch responses are drawn. The heave responses are non-dimensional values obtained by dividing the half of peak-to-peak values by the corresponding wave amplitude, and the pitch responses are the half of peak-to-peak values divided by the corresponding maximum wave slope. The heave responses do not have the resonance and in higher frequency from 6 to 10 rad/sec there are humps which are not visible in the pitch responses. And the distortion ratios, represented as dashed lines in figure, have somewhat large values in the range from 5 to 6 rad/sec, at which the responses are small. This means that the shape of motion is far from the sinusoidal shape, and the non-linearity dominates. Of course, for small wave amplitudes such as $kA=0.01, 0.05$, the behaviors of motion are nearly sinusoidal and the linearity dominates. The pitch responses become smaller as the wave amplitude goes large, and there is one resonance. The response near the resonance frequency is much affected by the wave amplitude. As shown in figure, the distortion ratios are small enough, so the behaviors of motion are nearly sinusoidal.

The mean sinkage and trim are shown in Fig.8. The mean values are non-dimensionalized by the wave amplitude for sinkage and by the wave slope for trim. Sign conventions are that the sinkage is positive when the craft goes up, and the trim is positive when the bow goes down. The sinkages are always negative, that is, the craft goes down when it meets the waves. The trend is that the sinkage goes down as the frequency goes high, while its behavior is different for the each wave system. Over nearly all the frequency range, the trim is positive, that is, the bow goes down. But in higher frequency over about 7 rad/sec, the trim becomes small.

In Fig.9, the vertical displacements at the bow and stern are drawn. The non-dimensionalizations are the same as in Fig.7. Seen in the figure, the vertical displacement at the bow have a quite large value near the resonance frequency, and this value is about three times greater than that of heave for a small wave. For a large amplitude wave, that is $kA=0.15$, the vertical displacement at the resonance goes down to about value 2. The distortion ratios are small for all frequency, this said that the vertical displacement at bow mainly affected by the pitch motion. At the stern, the vertical displacement is similar to that of heave except the fact that there is no hollow and hump, while the heave response has a hollow and hump at high frequency. And the responses for large amplitude waves such as $kA=0.1, 0.15$, are nearly constant over the range from 3 rad/sec to 8 rad/sec. These behaviors of the vertical displacement at the bow and stern are made intentionally in the design stage of the side hulls in order to lessen the motion at the stern so to provide the good condition for the propulsion device. So these behaviors may be different a little from one craft to another craft.

The vertical accelerations at the bow, stern, and midship are given in Fig.10. The vertical accelerations behave like the vertical displacements. At the bow and midship, there are two peaks at 3 rad/sec and 8 rad/sec, however at the stern, there is no peak and the acceleration level remains constant over large range of frequency. But remember that one wave system has a constant wave slope, in other words, the amplitude of one wave system decreases as the frequency increases. Similar to the case of displacement, the acceleration is greater at the bow and it is small at the stern. The distortion ratios are large over the frequency range from 2 rad/sec to 6 rad/sec, so in this range the shape of acceleration in time is far from the sinusoidal shape.

Let's consider the forces acting on the craft, the maximum wave slope is setting as $kA=0.1$. Fig.11(a) shows the hull forces, the static force is small compared with the other components. The forces due to the added mass and due to the change of added mass are comparable in the low and medium frequency region, but in high frequency region the forces due to the change of added mass are small compared with those of added mass. It seems that this fact can be applicable to a high speed planning craft. In Fig.11(b), the forces due to the pressures are drawn, the total pressure force mainly consists of the force due to the pressure in the cushion chamber, and that due to the pressure in the bag is negligible. Fig.11(c) shows the comparisons between the hull force and the pressure force. The mean force of the side hulls and the mean force due to the pressures behave opposite to each other, so the sum of mean forces remains constant, and the mean pressure force is larger than that of hulls. The mean pressure force is smaller than that of the steady state value, that is, the value with no wave. And the mean hull force which is the mean static force is larger than that of steady state value, this means that the sinkage takes place and the resistance of the craft will increase.

The moments acting on the craft are shown in Fig.12. Fig.12(a) shows the moments of the hulls. Opposite to the forces, the moment due to the statics is the largest. The moments due to the added mass and the change of the added mass are similar in magnitude, and the behavior is similar to the corresponding forces. In the Fig.12(b), the pressure moments are drawn. The moment due to the pressure in the bag is the main component. This is the phenomenon different from the case of forces in which the force due to the bag pressure is

the smallest. This is because that the bag is located at the stern, so the moment arm of the bag pressure force is large. Fig.12(c) shows the comparisons between the hull moment and the pressure moment. The mean values behave opposite to each other so the sum of two moments remains constant as in Fig.11(c). The magnitudes of the oscillating moments are comparable with each other, and near the resonance frequency the hull moment is larger, and in high frequency the pressure moment is larger. Considering that the moment due to the bag pressure is the main part of the pressure moment, the bag seems to play an important role in the pitch response of SES as expected.

3.2 Motions in Irregular Wave

All motions in irregular waves are calculated up to 110 second. Fig.13 – Fig.16 show the irregular motion characteristics varying the significant wave height $H_{1/3}$, and the calculations were made three times at each case. The solid lines in the figure are the fitting lines of the calculating points.

Fig.13 shows the ratio of the time of bow seal emergency to total time, and that of the bag fly. When the significant wave height is less than 1m, the bow seal always meets the free surface, and above this value the lowest point of the bow seal starts to move up and down the free surface. The time ratio is shown in figure. The fly of the stern bag takes place even on small significant wave height, this phenomenon is easy to happen because the bag flies if the pressure in the cushion chamber is high enough compared to the pressure in the bag. This time ratio can be made small if the pressure in the bag is increased by any means such as adopting the large fan to the stern bag and designing the feeding holes.

The mean sinkage and the mean trim are shown in Fig.14. As the significant wave height grows large, the mean sinkage and trim grows along with the wave height. For high wave height above 3m, the sinkage and the trim remain almost constant.

Fig.15 shows the change of the hull displacement. The mean displacement increases linearly when the significant wave height is less than 3m. For the wave height above 3m, the mean displacement is two times of the initial displacement, so the resistance increases according the increase of hull displacement.

The RMS values of acceleration at the bow, midship, and stern were drawn in Fig.16. The acceleration levels of midship and stern are about the same, and that of the bow is about two times larger than that of midship. The RMS accelerations increase rapidly in the range where the significant wave height is smaller than 1.5m. And in the range over about 2m, the accelerations increase slowly.

The power spectral density function of acceleration is shown in Fig.17. The significant wave height is 3m. The first peak is located at 0.4 Hz, and the second peak is at 1.2 Hz. The first peak occurs at the peak frequency of the wave spectrum, and the second peak occurs at the second resonance of the heave response shown in Fig.7. Comparing with Fig.10, the characteristics of the accelerations are somewhat alike that of regular waves.

4 Conclusions

In this paper, the heave and pitch motion in waves are studied. For doing this, the mathematical model for the deformation of the stern bag is investigated, and the hydrodynamic forces on the side hulls and the air flows are also investigated. The non-linear equations of motion including the heave, pitch, and 4 pressure variations are obtained. Solving the result equations of motion, the motion responses of SES in waves are studied. As a result, the following conclusions are drawn.

The mathematical model of the stern bag was derived, and the dynamical matching to the dynamics of the craft was done.

The non-linearity strongly appears in the pitch response rather than in the heave response. The resonance appears in pitch response, but there is no first resonance in heave motion.

The force due to the stern bag plays an important role in the pitch response, but in the heave response the effect is very small.

The force due to the added mass of the hulls has similar value in magnitude to the force due to the change of added mass.

In irregular waves, the motion characteristics change little when the significant wave height is larger than 3m.

The vertical acceleration of the bow is about two times larger than those of the midship and stern.

Further studies are required on the comparisons with the experimental studies and on the ride control systems.

References

- [1] Kaplan, P. et al., Dynamics and Hydrodynamics of Surface Effect Ships, *SNAME Trans.* vol.89, 1981
- [2] Murakami, T. & Yamakita, K., Prediction Method of Seakeeping Qualities of Surface effect Ship, *Symposium on the Prediction Method of Seakeeping of High-Speed Craft*, Japan, 1990
- [3] Yamakita, K., Design and Application of Ride Control System for 30 ton SES Test Craft, *SNAJ*, vol.169, 1991
- [4] Rhee, K.P. & Lee, G.J. & Hwang, J.H., Analysis of a PID Ride Control System for a Surface Effect Ship in Waves, *Proceedings HPV'92*, China, 1992

- [5] Hong, S.W. et al., Study of the Seakeeping Performance of Air Cushion Vehicle with Ride Control System, *Report No. UCE505-1568.D*, Korea Research Institute of Ships & Ocean Engineering, 1992
- [6] Martin, M., Theoretical Prediction of Motions of High-Speed Planing Boats in Waves, *JSR*, vol.22, No.3, 1978
- [7] Long-Wen, W., A Study on Motions of High Speed Planing Boats with Controllable Flaps in Regular Waves, *ISP*, vol.32, No.365, 1985
- [8] Kihara, K. & Takahashi, T., Prediction Method of Ship Motion and Acceleration of Monohull Type High-Speed Craft, *Symposium on the Prediction Method of Seakeeping of High-Speed Craft*, Japan, 1990
- [9] Ozawa, H. et al., On Dynamic Characteristics of SES Seal Systems, *SNAJ*, vol.158, 1986
- [10] Lee, G.J. & Rhee, K.P., A Deformation Model of a Bag-Finger Skirt and the Motion Response of an ACV in Waves, *SNAK*, vol.29, no.2, 1992
- [11] Lee, G.J., On the Hydrodynamic Forces acting on a Partially Submerged Bag, *SNAK*, vol.29, no.4, 1992
- [12] Lee, G.J., Effects of Air Compressibility on the Hydrodynamic Forces of a Bag, *SNAK*, vol.30, no.3, 1993

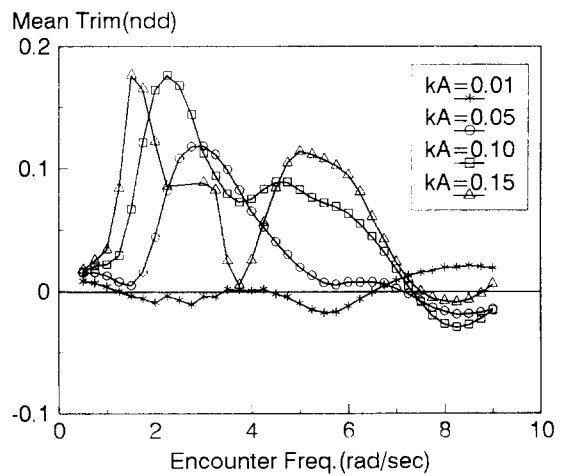
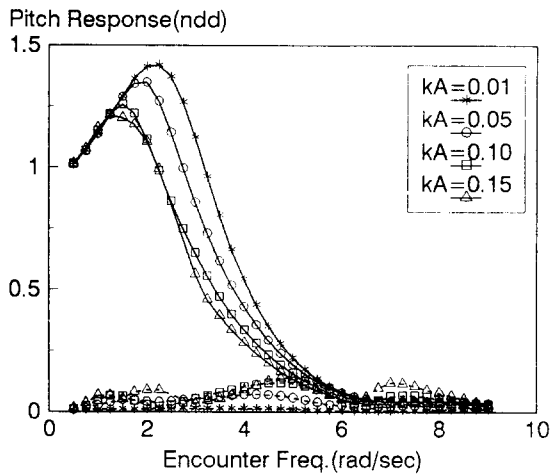
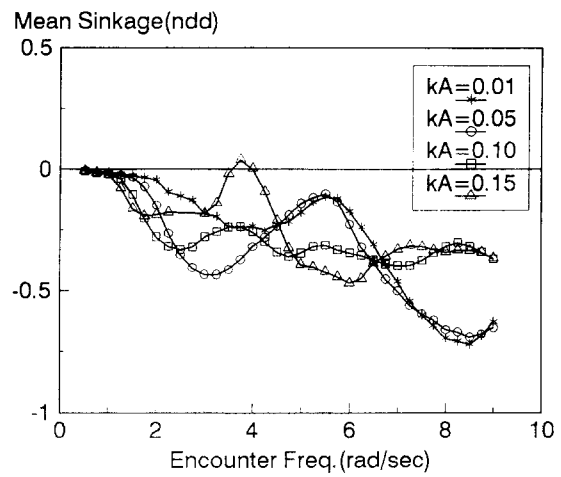
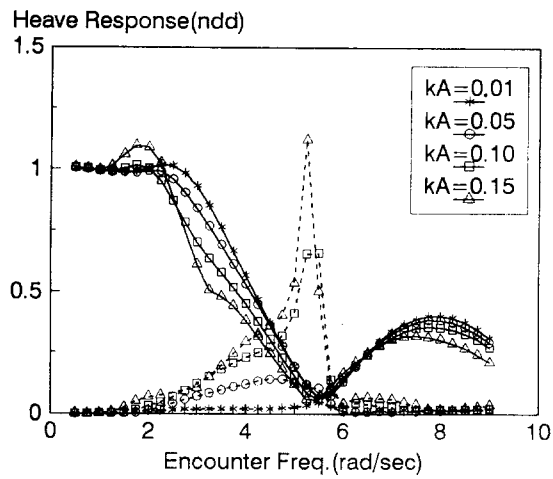


Figure 7: Heave and pitch responses for various wave systems. Solid lines are for the responses, and the dashed lines are for the distortion ratios.

Figure 8: Mean sinkage and trim for various wave systems.

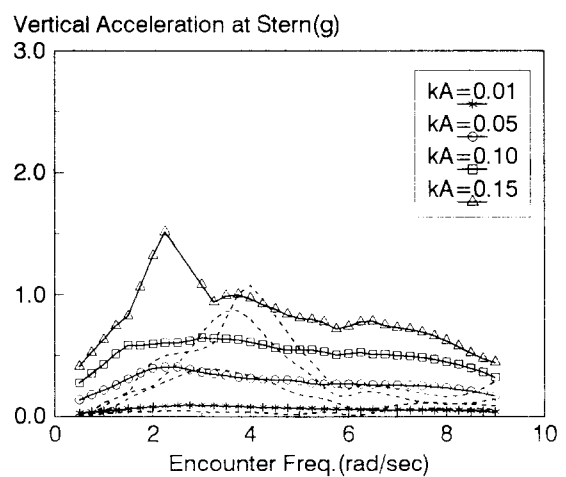
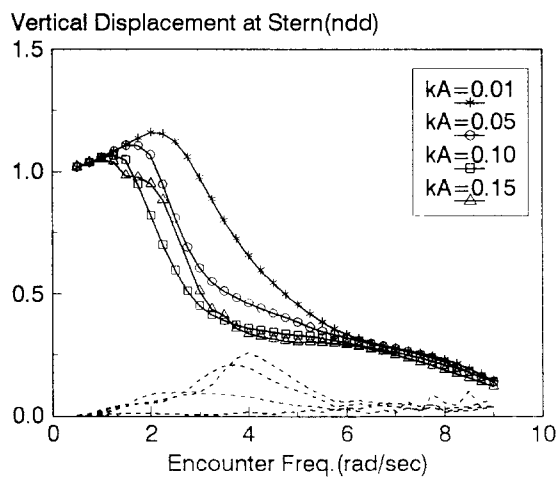
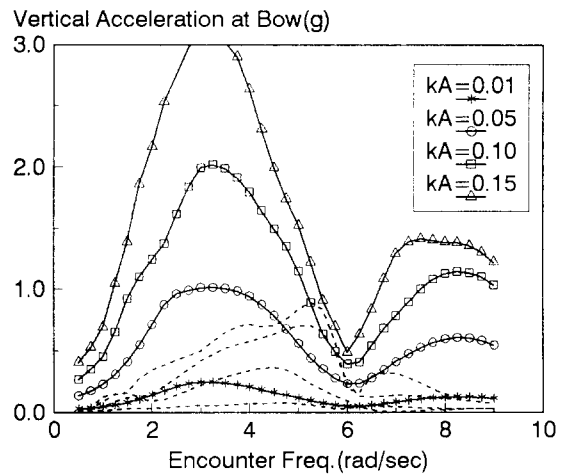
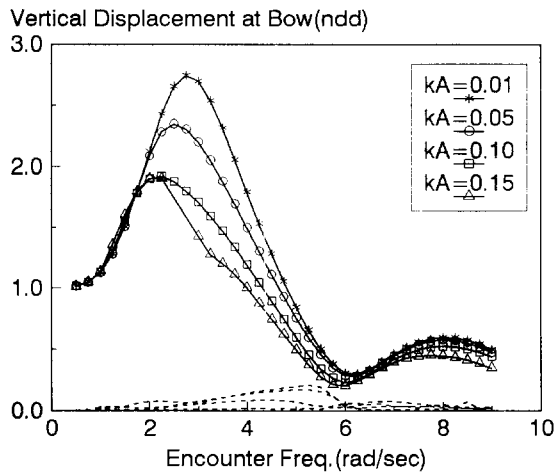
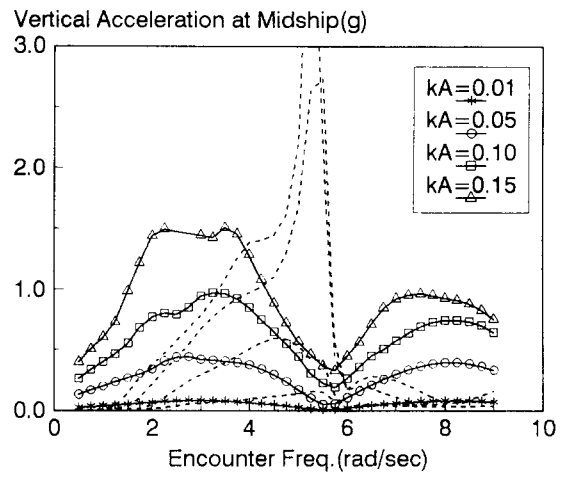
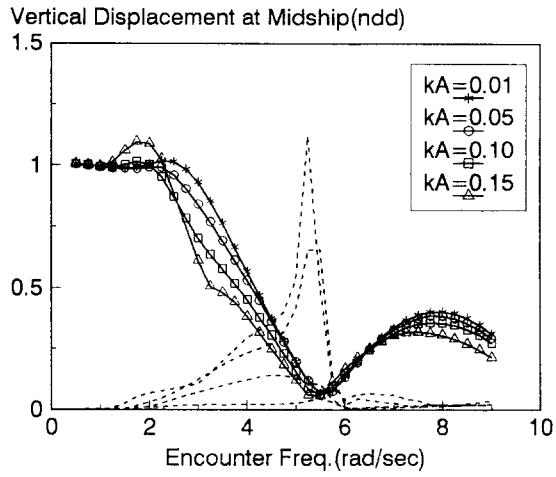


Figure 9: Vertical displacement at the bow and stern for various wave systems. Solid lines are for the displacements, and dashed lines are for the distortion ratios.

Figure 10: Vertical accelerations for various wave systems. Solid lines are for the accelerations, and dashed lines are for the distortion ratios, and g is the gravitational acceleration.

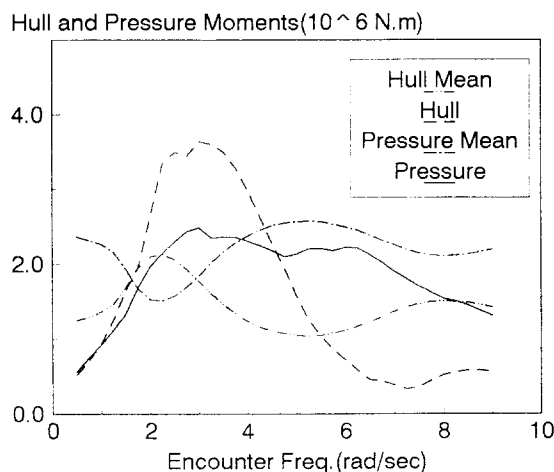
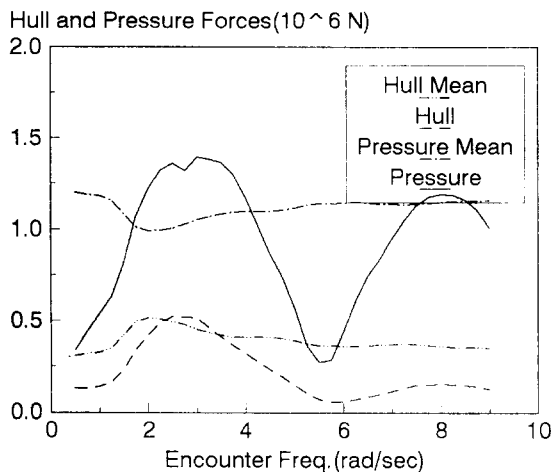
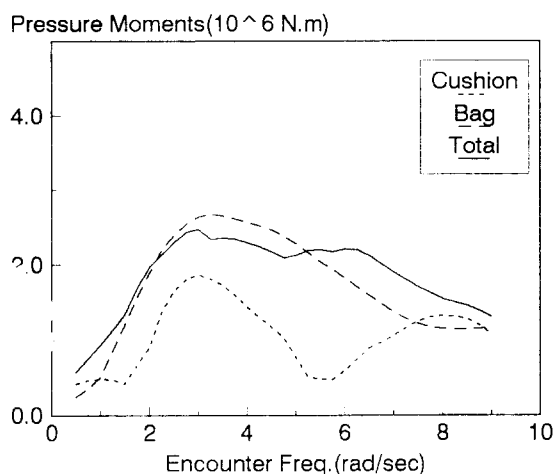
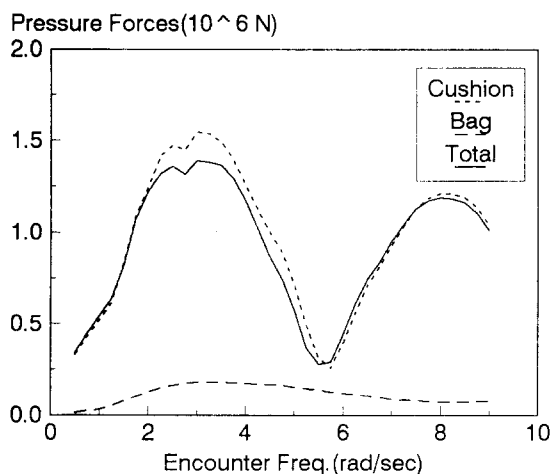
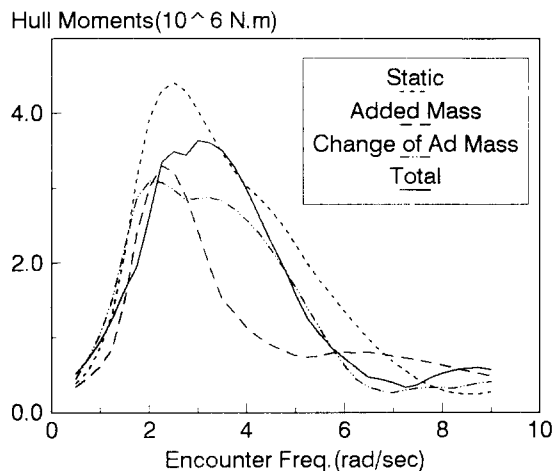
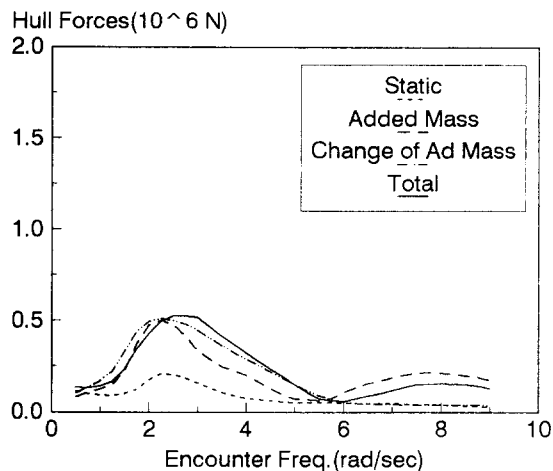


Figure 11: Forces acting on the hulls, forces due to the pressure, and comparison.

Figure 12: Moments acting on the hulls, moments due to the pressure, and comparison.

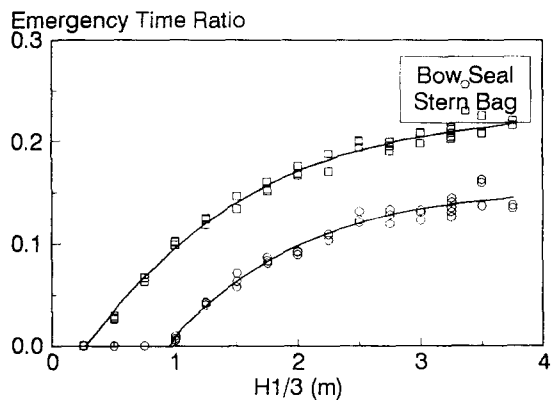


Figure 13: Ratio of the emergency time of the bow seal and stern bag to the total time.

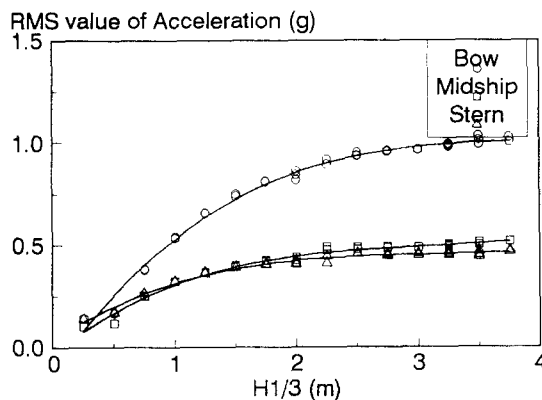


Figure 16: Root mean square value of the acceleration at the bow, midship, and stern.

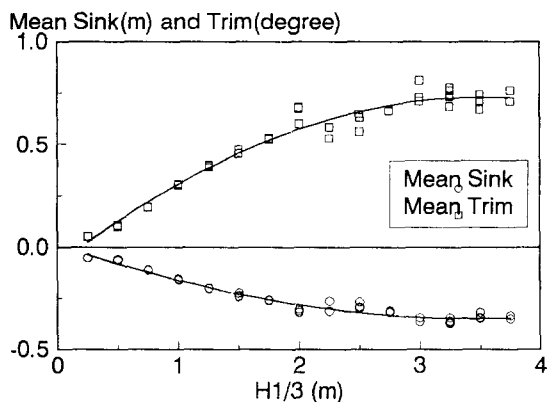


Figure 14: Mean sinkage and mean trim.

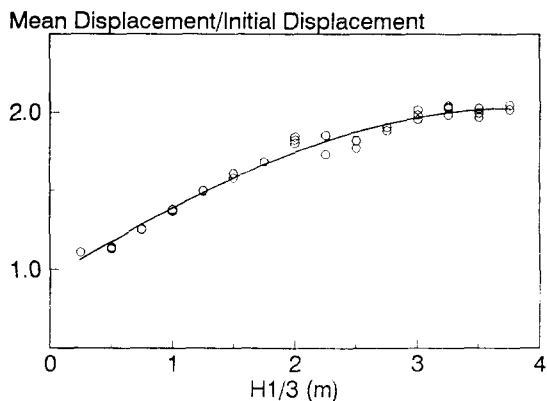


Figure 15: Ratio of the mean displacement to the initial displacement.

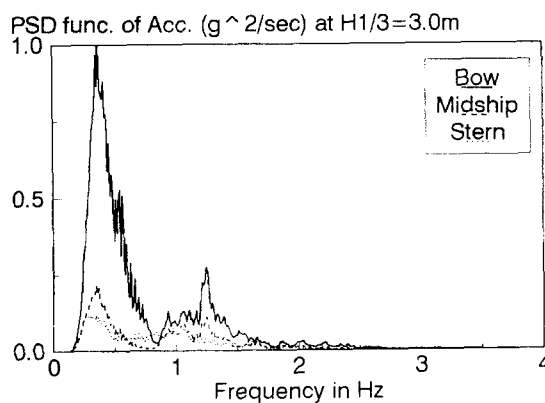


Figure 17: Power spectral density function of the acceleration at the bow, midship, and stern. The significant wave height is 3m.